

Bi-stability of micro-plates

A sensitive mechanism for differential pressure measurements

Sajadi, Banafsheh; Goosen, Johannes; Van Keulen, Fred

DOI

[10.1063/1.5003223](https://doi.org/10.1063/1.5003223)

Publication date

2017

Document Version

Final published version

Published in

Applied Physics Letters

Citation (APA)

Sajadi, B., Goosen, J., & Van Keulen, F. (2017). Bi-stability of micro-plates: A sensitive mechanism for differential pressure measurements. *Applied Physics Letters*, 111(12), Article 124101. <https://doi.org/10.1063/1.5003223>

Important note

To cite this publication, please use the final published version (if applicable). Please check the document version above.

Copyright

Other than for strictly personal use, it is not permitted to download, forward or distribute the text or part of it, without the consent of the author(s) and/or copyright holder(s), unless the work is under an open content license such as Creative Commons.

Takedown policy

Please contact us and provide details if you believe this document breaches copyrights. We will remove access to the work immediately and investigate your claim.

Bi-stability of micro-plates: A sensitive mechanism for differential pressure measurements

Banafsheh Sajadi,^{a)} Johannes (Hans) Goosen, and Fred van Keulen

Department of Precision and Microsystem Engineering, Faculty of Mechanical, Maritime and Materials Engineering, Delft University of Technology, 2628 CD Delft, The Netherlands

(Received 6 April 2017; accepted 4 September 2017; published online 19 September 2017)

The electrostatic instability (pull-in) of a flat electrode in a parallel plate capacitor has been shown to be highly sensitive to external mechanical loads such as pressure. In this paper, we substantiate the possibility of prompting additional unstable configurations in such a system, with a remarkable sensitivity to the applied pressure. This additional instability has significant advantageous properties for sensing purposes. In addition to the high sensitivity and robustness of the pull-in voltage measurements, it can be adjusted so that after the unstable configuration is met, a snap-through to a new stable configuration occurs. As a result of this bi-stable behavior, the contact between the electrodes, which is the main drawback of pull-in phenomena, will be easily avoided. The results of this paper particularly suggest the suitability of this mechanism for two different methods of pressure measurements. *Published by AIP Publishing.* [<http://dx.doi.org/10.1063/1.5003223>]

Electrostatic instability has been employed for both actuation and sensing in many electrostatic micro-electromechanical systems (MEMS).^{1–3} The latter typically consists of a simple parallel plate capacitor using at least one movable or flexible electrode. When an electric potential is applied to the capacitor, an attractive electrostatic load is induced between its electrodes, leading to deformation of the flexible electrode(s). The instability of parallel plate capacitors occurs due to the nonlinearities in the electrostatic load and the elastic structural response.⁴ At a critical deflection of the flexible electrode, the stiffness of the structure in the transverse direction vanishes and a small increase in the bias voltage, or an external load, leads to abrupt pull-in.⁵ When operating the micro- or nano-electro mechanical systems close to their critical (unstable) configurations, it is possible to benefit from their reduced stiffness and high sensitivity while still avoiding pull-in.^{6–8} It should be noticed that increasing the sensitivity by decreasing the stiffness will amplify the noise effects as well.

Although generally considered as a failure mechanism, pull-in is a unique feature of MEMS/NEMS devices,¹ and it can provide information on the mechanical and physical characteristics of the system.^{9,10} Hence, it can be used for measuring the mechanical properties of nano-structures,¹¹ sensing the adsorbate stiffness,¹² detecting gas,¹³ and measuring the residual stress in clamped structures.⁵ In addition, theoretical studies have shown that the pull-in voltage is highly sensitive to external mechanical loads applied to the electrode, such as pressure or in-plane tension,^{14–18} which suggests the pull-in instability as a potential mechanism for load sensing.

The pull-in instability as a sensing mechanism has a major problem. After pull-in, the contact between the electrodes causes failures including short circuits, sticking, and wear.^{4,19} If the sensor employs a bi-stable flexible electrode (such as an arched plate), after reaching the pull-in voltage, the electrode snaps to another stable configuration which is not in contact with the other electrode,^{20,21} and if the voltage is released, it

snaps back to its original configuration. Hence, the contact between the electrodes is avoided, and multiple measurements can be performed without failure. However, arched structures are relatively stiff compared to their equivalent flat plate, which in turn reduces their sensitivity as a sensor.

In this paper, we show that a capacitive pressure sensor, with a completely flat flexible electrode, is capable of exhibiting bi-stability, and a snap-through behavior after the instability is reached. This bi-stability can be achieved by proper tuning of the applied electrostatic potential and external pressure and is a potential proxy for the pressure. Such a sensor can benefit from a remarkable sensitivity and robustness of pull-in measurements and still avoid contact failure.

To confirm this argument, an analytical estimation and a finite element model are used to study the behavior of a capacitive pressure sensor with a very thin, circular, fully clamped plate as the flexible electrode. The schematic model is shown in Fig. 1. The radius of the flexible electrode is R , and its thickness is t . The Young's modulus and Poisson ratio of the plate are considered to be E and ν , respectively. The plate is suspended over a grounded electrode with a similar radius, and the gap between the two electrodes is d . As a test case, we consider $R = 100 \mu\text{m}$, $t = 0.2 \mu\text{m}$, $d = 2 \mu\text{m}$, $E = 80 \text{ GPa}$, and $\nu = 0.2$.

The flexible electrode is loaded with a differential pressure P , and an electric potential V_{dc} is applied to the

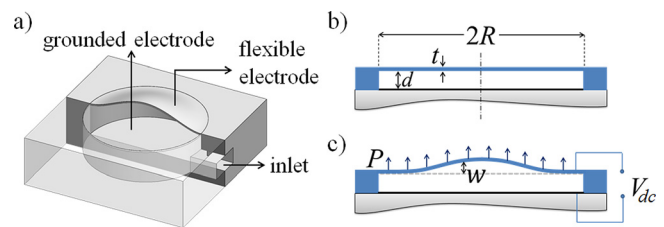


FIG. 1. (a) Schematic of the pressure sensor and its cross section, (b) undeformed configuration, and (c) deformed under combined electrostatic and differential pressure.

^{a)}Author to whom correspondence should be addressed: b.sajadi@tudelft.nl

electrodes. The principle of minimum total potential energy is employed to approximate the deflection in the equilibrium state. A simple approximate parametrized displacement field satisfying the kinematic boundary conditions is used for the mid-plane of the flexible electrode

$$\begin{aligned} w &= \xi_1 d(1 - \rho^2)^2, \\ u &= R\rho(1 - \rho)(\xi_2 + \xi_3\rho), \end{aligned} \quad (1)$$

where ρ is the non-dimensional radial coordinate, u and w are the radial and transverse displacement components, respectively, and ξ_i ($i=1-3$) is the generalized degrees of freedom. Using the Kirchhoff plate theory, the total potential energy of the system is expressed in terms of u and w and their derivatives. The total potential energy consists of four contributions associated with the electrostatics, the differential pressure, and the bending and stretching of the plate. Thus,

$$\begin{aligned} U &= -\pi\epsilon V_{dc}^2 R^2 \int_0^1 \frac{\rho d\rho}{d+w} - 2\pi PR^2 \int_0^1 w\rho d\rho \\ &+ \frac{\pi D}{R^2} \int_0^1 \left(\left(\frac{\partial^2 w}{\partial \rho^2} \right)^2 + \left(\frac{1}{\rho} \frac{\partial w}{\partial \rho} \right)^2 + \left(\frac{2\nu}{\rho} \frac{\partial w}{\partial \rho} \frac{\partial^2 w}{\partial \rho^2} \right) \right) \rho d\rho \\ &+ \frac{\pi Et}{(1-\nu^2)} \int_0^1 \left(\left(\frac{\partial u}{\partial \rho} + \frac{1}{2R} \left(\frac{\partial w}{\partial \rho} \right)^2 \right)^2 + \left(\frac{u}{\rho} \right)^2 \right. \\ &\left. + \frac{2\nu u}{\rho} \left(\frac{\partial u}{\partial \rho} + \frac{1}{2R} \left(\frac{\partial w}{\partial \rho} \right)^2 \right) \right) \rho d\rho, \end{aligned} \quad (2)$$

where ϵ is the electric permittivity of the dielectric between the electrodes and $D = \frac{Et^3}{12(1-\nu^2)}$ is the bending stiffness of the flexible plate.^{1,22} Note that the nonlinear terms due to the stretching and the non-uniformity of the electrostatic pressure are included in this formulation. By finding the stationary values of the total potential energy (U), we can determine the values of ξ_i in equilibrium states.

Due to the nonlinearity, the equilibrium path might exhibit unstable solution branches and limit points. The corresponding limit voltage(s) can be calculated analytically as a function of the applied pressure, by analyzing the determinant of the tangent operator ($[\frac{\partial U}{\partial \xi_i}]$). In fact, an equilibrium configuration is stable if the corresponding tangent operator is positive definite and unstable otherwise. The critical or limit points are the configurations at which the tangent operator is singular. To verify the accuracy of the analytical estimation, the commercial finite element software COMSOL was employed, and the worst case error was found to be less than 6% (see the [supplementary material](#) for details).

Figure 2 shows the obtained normalized deflection at the center of the flexible electrode (w/d), as a function of the normalized applied voltage, for three different differential pressures. The voltage is normalized with the limit (pull-in) voltage of the capacitor when no pressure is applied ($P=0$ Pa). In this case, the pull-in voltage is $V_p = 16.7$ V, and the midpoint of the thin plate can deflect up to 73% of the gap size before pull-in occurs. This difference with the engineering estimation (1/3 of the gap) occurs due to accounting for both the nonuniform electrostatic load and the geometrical *nonlinear* behavior of the micro-plate.¹⁹

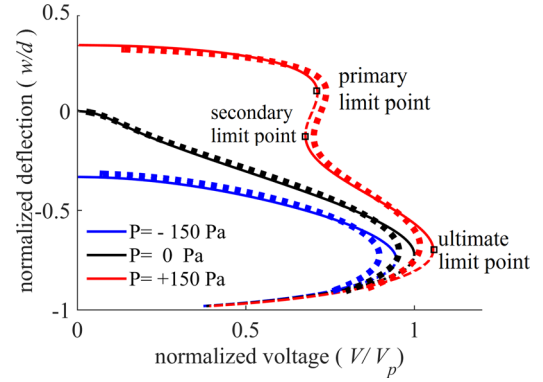


FIG. 2. The normalized deflection of the circular flexible electrode as a function of the normalized voltage, for different differential pressures: —, stable equilibrium; - - -, unstable equilibrium; and ■ ■ ■ ■, COMSOL simulations.

As Fig. 2 shows, a small pressure on the flexible electrode can significantly affect the shape of the equilibrium path. A non-zero mechanical pressure on the plate introduces an initial deflection. Obviously, the initial deflection depends on the amount and direction of the applied pressure. Second, *a differential pressure would influence the position and/or number of limit points* (i.e., the local maxima or minima of the voltage). When a negative (downward in Fig. 1) pressure is applied, the pull-in voltage drops and the critical deflection increases slightly, whereas the overall shape of the equilibrium path remains the same.

For positive pressures, however, the shape of the equilibrium path exhibits essential shape changes. As Fig. 2 indicates, now, the system might exhibit three critical points. One limit point occurs when the deflection of the plate is still in the positive direction (see Fig. 2). We refer to this point as the *primary* limit point. This limit point only occurs if the pressure is higher than a certain amount. The primary critical deflection varies between 0 and 50% of the initial gap size, though in the positive direction. Another limit point corresponds to a local minimum in the applied voltage. This point will be referred to as the *secondary* limit point. The last limit point is near the pull-in voltage when no pressure is applied, only at a slightly different voltage and deflection. We refer to this point as the *ultimate* limit point. At the ultimate limit point, the deflection of the plate is 65–73% of the initial gap size, depending on the applied pressure.

In order to understand the underlying physics of existence of such bi-stability, in the presence of pressure, the generalized electrostatic and restoring loads are illustrated in Fig. 3. The loads are obtained as the derivative of the associated potential energy with respect to the transverse deflection and divided by the area (πR^2). Clearly, when the electrostatic load and restoring loads are equal, the system is in equilibrium.

Due to geometric spring hardening, the elastic restoring load is a cubic function of the deflection. First, consider the case where no pressure is applied on the system [i.e., $P=0$ in Fig. 3(a)]. If the applied voltage is smaller than the pull-in voltage, at two configurations, the electrostatic and elastic restoring loads are equal. One solution is a stable equilibrium, and the other one is unstable. If the applied voltage is higher than the pull-in voltage, the electrostatic load is always larger

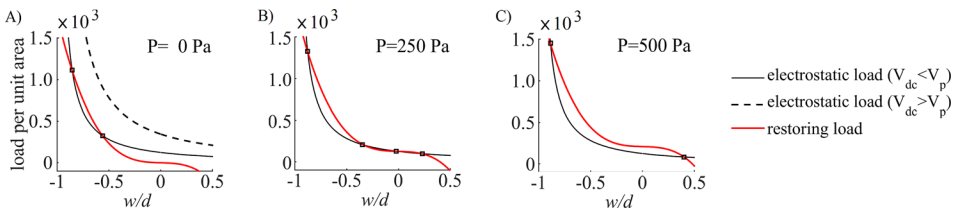


FIG. 3. The electrostatic and the restoring loads per unit area as a function of deflection for (a) $P = 0$, (b) $P = 250$ Pa, and (c) $P = 500$ Pa. Equilibrium configurations are indicated with dots (■).

than the elastic restoring load. Therefore, no equilibrium solution can be found.

Clearly, a differential pressure in the opposing direction of the electrostatic load adds up to the restoring loads. Therefore, the restoring load is shifted up, and in that case, instead of two points, the plate might have four equilibrium configurations, two of which would be stable [see Fig. 3(b)]. It should be noticed that the existence of two additional solutions is only due to geometrical nonlinearity of the clamped plate. In fact, if the stiffness was constant, the elastic restoring load was linear and the additional solutions would have not been observed. By increasing the pressure further, again only two equilibrium solutions can be found [see Fig. 3(c)].

If we increase the voltage around the primary limit point or decrease the voltage around the secondary limit point, the electrode snaps from one stable configuration to the other. In fact, after the system passes the primary limit point, the post-instability behavior strongly depends on the applied pressure (see Fig. 4). For smaller pressures, a snap-through to another stable state is observed (e.g., $P = 200$ Pa in Fig. 4), whereas, for higher pressures, the primary limit voltage might exceed the ultimate pull-in voltage and, thus, a small perturbation— increase of voltage for example—can lead to total failure (see $P = 400$ Pa in Fig. 4). For very large pressures, the secondary and ultimate limit points vanish.

The deflection and voltage at the primary limit point can provide information on the mechanical load applied to the structure. Thus, a measurement of the primary limit point can serve as a proxy for the applied load. In order to demonstrate the suitability of the primary instability for load measurements, the sensitivity of the primary limit voltage to an applied differential pressure is studied. Figure 5 shows how the primary and ultimate limit voltages change with the applied pressure. It can be seen that both limit voltages are very sensitive to any change in pressure. For negative (downward) pressures, there is a monotonic near-linear relationship between the pressure and the ultimate pull-in voltage.

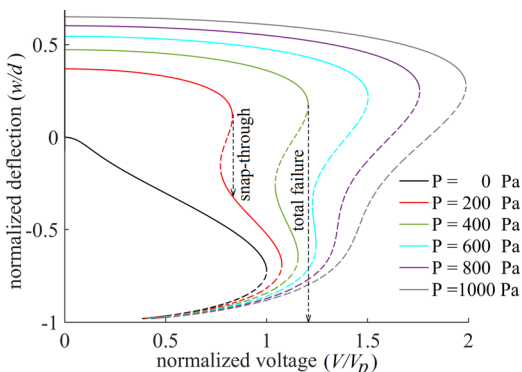


FIG. 4. The equilibrium path of the midpoint of the circular flexible electrode for different differential pressures: —, stable solution; - - -, unstable solution.

For positive (upward) pressures, a primary limit point exists and the corresponding voltage monotonically increases with the initial pressure, albeit at a much higher rate. Notice that the sensitivity of the primary limit voltage exceeds 25 mV Pa^{-1} for the pressure changes, which is equivalent to a sensitivity of nearly 0.95 mV nm^{-1} for deflection. This number is clearly just for the proposed geometry and material properties. However, it shows the potential of the primary instability in comparison to the pull-in mechanism for pressure measurements. In the specified range of pressure in Fig. 5, the primary limit voltage is smaller than the ultimate limit voltage, and thus, only in this range, snap-through may occur.

It should be noticed that although the snap-through was illustrated for constant pressure and a sweep over voltage, a similar behavior is noticed if the voltage is preserved and the pressure is varied. As an example, the deflection of the center of the flexible electrode for a constant voltage (13.9 V) below the pull-in voltage is shown in Fig. 6. The associated limit points (primary, secondary, and ultimate pull-in) are shown in this figure. If the pressure is increased around the secondary limit point or decreased around the primary limit point, the micro-plate snaps from one stable branch to the other.

The noticed snap-through behavior can be achieved only for a certain combinations of pressure, radius, thickness, and material properties, which can be identified by both the analytical and finite element models. For instance, for the assumed material and radius ($100 \mu\text{m}$), the admissible range of pressure as a function of thickness is shown in Fig. 7. If the applied differential pressure is too small, the primary limit point does not exist. On the other hand, if the applied differential pressure is too high, the primary limit voltage would exceed the ultimate pull-in voltage. In such a case, the primary instability leads to a failure without snapping to a new stable configuration. Evidently, the snap-through is a dynamic

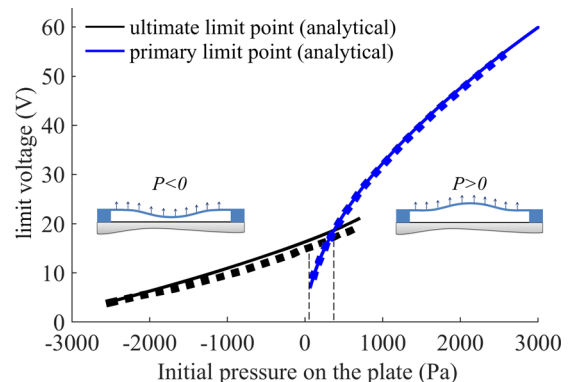


FIG. 5. Ultimate and primary limit voltages as functions of the differential pressure; the primary and ultimate limit voltage are highly sensitive to the pressure; —, analytical solution; and ■■■■, COMSOL simulations.

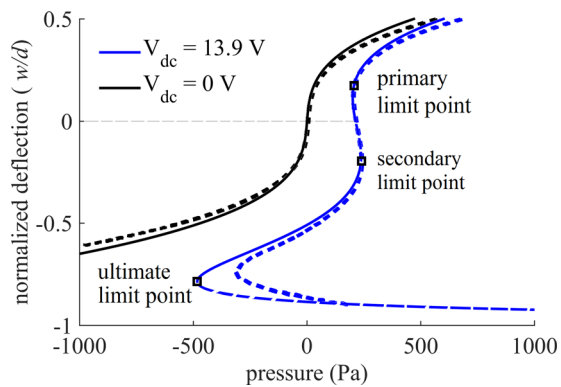


FIG. 6. The deflection in the center of the flexible electrode as a function of applied pressure, when voltage is kept constant; —, stable solution; - - -, unstable solution; and ■■■■, COMSOL simulations.

process, and when the flexible plate snaps from an unstable to a stable configuration, it has a nonzero velocity. To ensure that the ultimate limit point is not passed in this process, the total potential energy in both primary and ultimate limit points needs to be compared. In fact, the total potential at the primary limit point should be less than that at the ultimate limit point. The graphs in Fig. 7 are obtained based on this criterion. It is worth to mention that the pressure range for the existence of snap-through increases monotonically with the Young's modulus of the micro-plate, and it increases with a decrease in the radius. In fact, to benefit from the bi-stability of a micro-plate in a range of pressure, the proper thickness and radius of the flexible electrode shall be selected.

To employ the primary instability for sensing pressure, two techniques can be envisaged. The first is to subject the sensor to the measurand pressure and then ramp up the voltage to the primary limit voltage. This unstable point can be detected by a sudden change in capacitance (which for a controlled voltage will be detectable in current) or other measurement methods. Then, the corresponding pressure can be calculated. The second possible method would be a binary mechanism for detecting a certain differential pressure. In this method, the voltage is kept *close* to the primary (or secondary) limit voltage of the target pressure. Then, if the pressure drops (or inclines) to less (or more) than the target pressure, the system snaps. Hence, a precise binary mechanism for pressure measurement will be achieved.

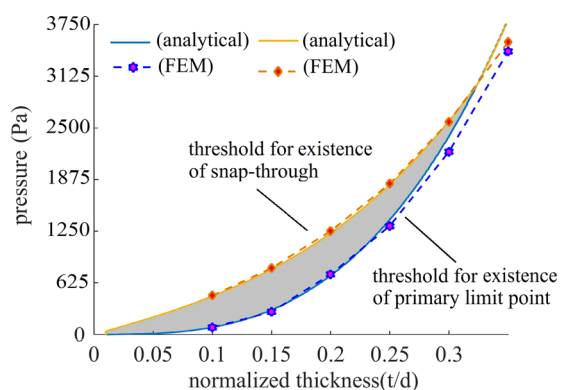


FIG. 7. The admissible region (gray area) for the existence of the primary limit point and the snap-through.

It should be mentioned that in practice, two factors of noise and imperfections can disturb the performance of the present sensor. Noise can determine the limit of detection (resolution) of the measurand.²⁴ Moreover, when the measurement is performed close to an unstable configuration, noise can introduce small vibrations around each stable equilibrium state, or large perturbations, allowing for jumps.²³ To evaluate the robustness of each stable configuration, we performed a series of dynamic transient analyses. The results indicate that compared to pull-in voltage measurements, a stochastic source of energy can more easily lead to an early jump before the primary limit point is reached. Furthermore, based on a preliminary calculation, a significantly low detection limit of 0.1 Pa is obtained for this sensor (see the [supplementary material](#) for the discussion on noise).

Imperfection and initial deflection can also significantly affect the stability of the micro-plate. Hence, this influence has been investigated using the COMSOL model. Initial deflections have been modeled similar to the first two buckling modes of a circular micro-plate as the most influential imperfections for its stability.²⁵ The results indicate that micro-plates with large symmetric initial deflections (for this case, with a maximum deflection larger than 0.15 times the distance between the electrodes) are inherently bi-stable. Moreover, *a-symmetric* initial deflections cause a noticeable change in the deformation of the system. However, such an initial deflection, if relatively small, only shifts the required pressure range for snapping behavior.

In summary, the nonlinearities of the elastic potential and electrostatic field can be used to tune the equilibrium curve of a flat flexible electrode and its instabilities. As a result, the flexible electrode can exhibit a primary instability and a snap-through behavior before the electrostatic pull-in occurs. The noticed primary instability is significantly sensitive to pressure. Therefore, it can be used as a sensing mechanism for highly sensitive pressure measurements. Moreover, such a measurement can benefit from snap-through behavior which prevents the system from failure. Although this mechanism does not allow for continuous sensing methods, it benefits from the simplicity of pull-in voltage measurements. The primary limit voltage of a pressure loaded parallel plate capacitor is potentially a suitable mechanism for sensing other types of mechanical loads such as surface stress or in-plane residual stress.

See [supplementary material](#) for details of COMSOL simulations and considerations on the effects of noise.

This work was supported by NanoNextNL of the Government of the Netherlands and 130 partners.

¹W.-M. Zhang, H. Yan, Z.-K. Peng, and G. Meng, *Sens. Actuators, A* **214**, 187 (2014).

²A. H. Nayfeh, M. I. Younis, and E. M. Abdel-Rahman, *Nonlinear Dyn.* **48**, 153 (2007).

³J. Seeger and B. E. Boser, *J. Microelectromech. Syst.* **12**, 656 (2003).

⁴W.-C. Chuang, H.-L. Lee, P.-Z. Chang, and Y.-C. Hu, *Sensors* **10**, 6149 (2010).

⁵D. Elata and S. Abu-Salih, *J. Micromech. Microeng.* **15**, 921 (2005).

⁶A. Jain, P. R. Nair, and M. A. Alam, *Proc. Natl. Acad. Sci.* **109**, 9304 (2012).

- ⁷D. Southworth, L. Bellan, Y. Linzon, H. Craighead, and J. Parpia, *Appl. Phys. Lett.* **96**, 163503 (2010).
- ⁸V. Kumar, J. W. Boley, Y. Yang, H. Ekowaluyo, J. K. Miller, G. T.-C. Chiu, and J. F. Rhoads, *Appl. Phys. Lett.* **98**, 153510 (2011).
- ⁹Q. Zou, Z. Li, and L. Liu, *Sens. Actuators, A* **48**, 137 (1995).
- ¹⁰S. Saghir and M. I. Younis, *Int. J. Non-Linear Mech.* **85**, 81 (2016).
- ¹¹H. Sadeghian, C.-K. Yang, H. Goosen, P. J. F. Van Der Drift, A. Bossche, P. J. F. French, and F. Van Keulen, *Appl. Phys. Lett.* **94**, 221903 (2009).
- ¹²H. Sadeghian, H. Goosen, A. Bossche, and F. van Keulen, *Thin Solid Films* **518**, 5018 (2010).
- ¹³M. Khater, "Use of instabilities in electrostatic micro-electro-mechanical systems for actuation and sensing," Ph.D. thesis, UWSpace, Waterloo, Ontario, Canada.
- ¹⁴A. Sharma and P. J. George, *Sens. Actuators A: Phys.* **141**, 376 (2008).
- ¹⁵J. Lardis, M. Berthillier, and M. L. Bellaredj, "Smart Sensors, Actuators, and MEMS V," *Proc. SPIE* **8066**, 80661N (2011).
- ¹⁶S. Krylov and S. Seretensky, *J. Micromech. Microeng.* **16**, 1382 (2006).
- ¹⁷A. Nabian, G. Rezazadeh, M. Haddad-derafshi, and A. Tahmasebi, *Microsyst. Technol.* **14**, 235 (2008).
- ¹⁸X. L. Jia, J. Yang, and S. Kitipornchai, *Acta Mech.* **218**, 161 (2011).
- ¹⁹L.-D. Liao, P. C. Chao, C.-W. Huang, and C.-W. Chiu, *J. Micromech. Microeng.* **20**, 025013 (2010).
- ²⁰L. Medina, R. Gilat, B. Ilic, and S. Krylov, *Sens. Actuators, A* **220**, 323 (2014).
- ²¹K. Das and R. C. Batra, *Smart Mater. Struct.* **18**, 115008 (2009).
- ²²M. Amabili, *Nonlinear Vibrations and Stability of Shells and Plates* (Cambridge University Press, 2008).
- ²³V. Lucarini, D. Faranda, and M. Willeit, *Nonlinear Processes Geophys.* **19**, 9 (2012).
- ²⁴B. Gabrielson, *IEEE Trans. Electron Devices* **40**, 903 (1993).
- ²⁵B. Budiansky, *Adv. Appl. Mech.* **14**, 1 (1974).